Journal of Statistical Physics, Vol. 62, Nos. 5/6, 1991

Macrotransport Processes: Brownian Tracers as Stochastic Averagers in Effective-medium Theories of Heterogeneous Media

Howard Brenner[1]

Received February 5, 1990; final March 27, 1990

Macrotransport processes (generalized Taylor dispersion phenomena) constitute coarse-grained descriptions of comparable convective-diffusive-reactive microtransport processes, the latter supposed governed by microscale linear constitutive equations and boundary conditions, but characterized by spatially nonuniform phenomenological coefficients. Following a brief review of existing applications of the theory, we focus—by way of background information—upon the original (and now classical) Taylor–Aris dispersion problem, involving the combined convective and molecular diffusive transport of a point-size Brownian solute "molecule" (tracer) suspended in a Poiseuille solvent flow within a circular tube. A series of elementary generalizations of this prototype problem to chromatographic-like solute transport processes in tubes is used to illustrate some novel statistical-physical features. These examples emphasize the fact that a solute molecule may, on average, move axially down the tube at a different mean velocity (either larger or smaller) than that of a solvent molecule. Moreover, this solute molecule may suffer axial dispersion about its mean velocity at a rate greatly exceeding that attributable to its axial molecular diffusion alone. Such "chromatographic anomalies" represent novel macroscale nonlinearities originating from physicochemical interactions between spatially inhomogeneous convective-diffusive-reactive microtransport processes.

KEY WORDS: Brownian motion in flowing/reacting systems; chromatography; porous media, transport processes in; Taylor dispersion theory, generalized; transport processes, micro- to macroscale transition.

1. INTRODUCTION

The research reviewed herein builds upon a scheme initiated more than 30 years ago by Taylor[1,2] and more firmly established by Aris,[3]

[1] Department of Chemical Engineering, Massachusetts Institute of Technology, Cambridge, Massachusetts 02139.

0022-4715/91/0300-1095$06.50/0

originally relating to the convective flow and dispersion of a soluble solute dissolved in a solvent undergoing Poiseuille flow in a circular tube. It is well known[4] that such a transport process is governed at the microscale by a convective-diffusion equation, involving radial, azimuthal, and axial transport of the solute within the tube. Taylor set himself the problem of *coarse graining* this equation, so as to describe only the mean, *axial* transport of solute down the tube, which is normally the only process of physical interest in applications. In bringing this quest to fruition he paved the way for an entirely new field—namely generalized Taylor dispersion theory or, as it has more recently come to be called (in a somewhat broader context), *macrotransport processes.*

Macrotransport processes provide a robust scheme for the study of dispersion phenomena arising from solute-velocity (and other phenomenological-coefficient) inhomogeneities in convective-diffusive transport processes. Since its original paradigmatic presentation,[5,6] additional physical elements have been incorporated into the theory, followed by successful application to a wide variety of transport problems. These include: (i) sedimentation of nonspherical particles[7,8]; (ii) dispersion accompanying solute flow through porous media (unconsolidated,[9] consolidated[10]); (iii) surface transport[11,12]; (iv) direct "coupling" effects,[13] which later enabled the study of the transport of flexible bodies and chains of interacting Brownian particles without having recourse to *ad hoc* preaveraging schemes[14,15]; (v) time-periodic nonunidirectional flows[16-18]; (vi) cellular flows characterized by a vortical microscale flow with no net macroscale flow[19,20]; (vii) chemically reactive[21-23] and aerosol filtration[24] systems, involving nonconserved Brownian tracers; (viii) effects of finite-size particles applied to chromatographic separation processes[25-27]; (ix) turbulent flow fields[28]; and (x) dispersion of "momentum tracers" in relation to the rheology of suspensions.[29]

An attractive feature of the general scheme is that it confers a unified, indeed paradigmatic, structure upon the analysis of an apparently widely-disparate class of physical problems, albeit those governed by *linear* constitutive equations and boundary conditions. The heterogeneous nature of the audience for whom this presentation is intended excludes entering into the details[2] of the paradigm,[5,6] and its extension to chemically reactive systems.[21-23] Moreover, in the limited time (and space) available we can do little more than enter into a few elementary examples illuminating several of the useful (and interesting) results obtained to date. In this context we have chosen to focus exclusively upon the role of *macrotransport*

[2] In the nonreactive case, the most probing examination of the fundamental paradigms of macrotransport processes will be found in the analysis of Frankel and Brenner.[30]

processes in rationalizing a variety of chromatographic-type concepts. These involve calculations of the mean velocity $\bar{U}^*$ and dispersivity $\bar{D}^*$ of a convected Brownian solute through capillary tubes (and, concomitantly, capillary-tube models of packed beds), including the case of chemically reactive solutes undergoing first-order irreversible reactions—for which a third macrotransport coefficient, the solute's volumetric reactivity $\bar{K}^*$, is required.[21-23]

2. THE TAYLOR–ARIS[1-3] PROBLEM

2.1. Convection and Diffusion of a Solute in a Poiseuille Flow. Microtransport Equations

Referring to Fig. 1, consider the Poiseuille flow

$$v(r) = 2\bar{V}[1 - (r/r_o)^2] \tag{2.1}$$

of an incompressible viscous fluid (the "solvent") at mean velocity

$$\bar{V} = \frac{1}{\pi r_o^2} \int_0^{2\pi} \int_0^{r_o} v(r) r \, dr \, d\phi \tag{2.2}$$

through an infinitely long circular capillary tube of radius r_o. Imagine that at time $t = 0$ a single point-size Brownian solute "molecule," "particle," or "corpuscle" (hereafter collectively referred to as the "tracer") is introduced into the flowing solvent at the point (r', ϕ', z'), where (r, ϕ, z) constitute a

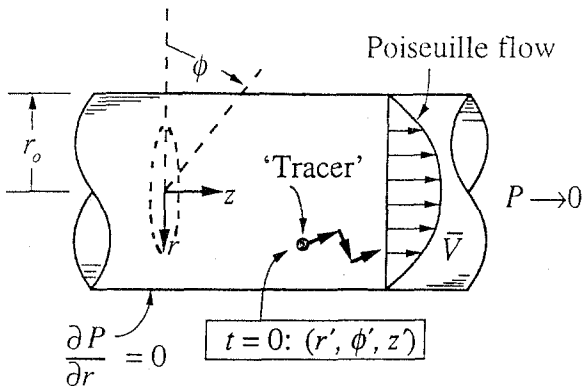

Fig. 1. Poiseuille flow of a viscous solvent at mean velocity $\bar{V}$ through an infinitely long circular capillary tube of radius r_o. At time $t = 0$ a point-size solute "molecule" (tracer) is introduced into the flowing fluid at the point (r', ϕ', z') without disturbing the flow.

system of circular cylindrical coordinates spanning the range ($0 \leqslant r < r_o$, $0 \leqslant \phi < 2\pi$, $-\infty < z < \infty$). At the continuum-mechanical level of description, subsequent transport of this tracer for times $t > 0$ occurs partly by convection wherein it is passively carried along piggy-back style at velocity $v(r)$ by the flowing solvent, and partly by diffusion (with molecular or Brownian diffusivity D) owing to the tracer's Brownian motion through the solvent.

The ensuing stochastic microscale tracer transport process can be described by the (conditional) probability density[5,6] $P \equiv P(r, \phi, z, t \mid r', \phi', z')$ that the tracer is present at time t at the point (r, ϕ, z) given its initial introduction into the system at time $t = 0$ at the point (r', ϕ', z'). Since the tracer is necessarily a conserved entity (at least in the nonreactive case under discussion here), it is necessarily present *somewhere* within the tube with probability one for all $t \geqslant 0$, whence P satisfies the normalization condition

$$\int_{-\infty}^{\infty} \int_0^{2\pi} \int_0^{r_o} Pr \, dr \, d\phi \, dz = \begin{cases} 1 & (t \geqslant 0) \\ 0 & (t < 0) \end{cases} \tag{2.3}$$

The conditional probability density P governing the tracer's microtransport process satisfies the following microscale convective-diffusive, initial- and boundary-value problem[5]:

$$\frac{\partial P}{\partial t} + v(r) \frac{\partial P}{\partial z} = D \nabla^2 P \tag{2.4}$$

$$P = \begin{cases} r^{-1} \delta(r - r') \, \delta(\phi - \phi') \, \delta(z - z') & (t = 0) \quad (2.5a) \\ 0 & (t < 0) \quad (2.5b) \end{cases}$$

$$\partial P / \partial r = 0 \qquad \text{at} \quad r = r_o \tag{2.6}$$

$$P \to 0 \qquad \text{as} \quad |z - z'| \to \infty \tag{2.7}$$

with δ the Dirac delta function. The implicit unit coefficient multiplying the right-hand side of (2.5a) derives from the unit normalization condition (2.3). Equation (2.6) arises from the impenetrability of the tube wall to both the solute and solvent, and represents a zero-valued normal flux condition imposed upon the solute. The spatial attenuation (2.7) of the far-field probability density toward zero is assumed to be faster than algebraic so as to assure that the integrals defining the axial moments

$$M_m \overset{\text{def}}{=} \int_{-\infty}^{\infty} \int_0^{2\pi} \int_0^{r_o} (z - z')^m \, Pr \, dr \, d\phi \, dz \tag{2.8}$$

($m = 0, 1, 2, \ldots$) are convergent for all m.

The initial- and boundary-value problem (2.4)–(2.7) posed for the solute's microprobability field P possesses a unique solution. Because of the nonconstancy of the phenomenological function $v(r)$ appearing in the convective term of the solute conservation continuity equation (2.4), this solution must be obtained numerically rather than analytically. Given the computational capacities and speed of modern computers, this would not be a difficult task—though the numerical solution would be specific to the specified initial tracer position (r', ϕ', z'); that is, a different numerical solution would be required for each different initial position.

2.1.1. Total (Conditional) Areal Probability Density Field[3] $\bar{P}(z, t)$. In any event, such exhaustively detailed information as would be embodied in the microsolution $P(r, \phi, z, t)$—numerically or otherwise—is rarely, if ever, required in practice. Rather, the quantity of usual interest in applications is the quantity

$$\bar{P} \overset{\text{def}}{=} \int_0^{2\pi} \int_0^{r_o} Pr \, dr \, d\phi \tag{2.9}$$

Modulo a factor of $1/\pi r_o^2$, $\bar{P}$ represents the area-average probability density over the cross section $z = \text{const}$. Obviously, $\bar{P}$ can be computed numerically from comparable numerical knowledge of P, although again the result would be specific to the initial tracer position (r', ϕ', z').

To the extent that knowledge of $\bar{P}$ is all that is required in practice, one is completely done with the physical problem at this stage. Unfortunately, such strictly numerical knowledge—while perhaps useful in parametric engineering design studies—rarely furnishes useful conceptual insights into the overall, *macroscale* physical phenomena arising from interactions existing between microscale convective and diffusive solute transport mechanisms. Moreover, the computation of $\bar{P}$ via this "first-principles" scheme is very wasteful of computer resources in the sense that having expended considerable effort to first compute the microfield $P(r, \phi, z, t)$, much of this detailed information is effectively discarded when the latter is coarse grained during the integration step (2.9) leading to $\bar{P}(z, t)$.

2.2. Macrotransport Processes

Given the preceding remarks, it is natural to inquire as to whether a more insightful and computer-resource-effective scheme or paradigm exists for (rigorously) proceeding from the specified microscale parameters and

[3] Here and throughout, we shall suppress the terms (r', ϕ', z') that would otherwise appear in the arguments of P and $\bar{P}$.

input data depicted in Fig. 2 to the desired coarse-grained field $\bar{P}(z, t)$. This important question was answered in the affirmative by Taylor[1,2] more than 30 years ago, with a major conceptual assist from Aris,[3] leading to what is today called Taylor dispersion theory. In particular, Taylor was able to show that if one is interested only in the asymptotic, long-time *macroscale* distribution $\bar{P} \equiv \bar{P}(z, t)$ for times t satisfying the dimensionless inequality

$$Dt/r_o^2 \gg 1 \tag{2.10}$$

then $\bar{P}$ itself obeys a (one-dimensional, macroscale) convective-"dispersion" *macrotransport equation*,

$$\frac{\partial \bar{P}}{\partial t} + \bar{U}^* \frac{\partial \bar{P}}{\partial z} \simeq \bar{D}^* \frac{\partial^2 \bar{P}}{\partial z^2} \tag{2.11}$$

possessing constant macroscale phenomenological coefficients $\bar{U}^*$ and $\bar{D}^*$. The latter are respectively given by

$$\bar{U}^* = \bar{V} \tag{2.12}$$

and

$$\bar{D}^* = D + \frac{r_o^2 \bar{V}^2}{48D} \tag{2.13}$$

and are thus expressed in terms of the prescribed input parameters r_o, $\bar{V}$ and D (cf. Fig. 2) governing the comparable microtransport problem defining P. Not only are these two coefficients independent of spatial position z and time t, but, equally important, they are independent of the initial (microscale) position (r', ϕ', z').

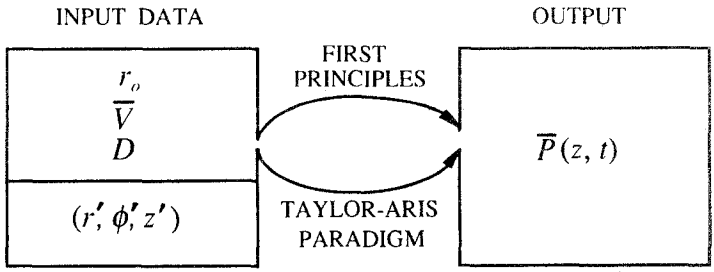

Fig. 2. Two (equally rigorous) alternative schemes for proceeding from the specified microscale parameters and initial data to the area-average solute concentration $\bar{P}$.

To obtain the mean field $\bar{P}$, one has thus only to solve the constant-coefficient macrotransport equation (2.11) subject to the far-field boundary condition

$$\bar{P} \to 0 \qquad \text{as} \quad |z - z'| \to \infty \tag{2.14}$$

and macroscale initial condition

$$\bar{P} = \begin{cases} \delta(z - z') & (t = 0) \\ 0 & (t < 0) \end{cases} \tag{2.15}$$

The solution,

$$\bar{P} \simeq \bar{P}(z - z', t) \equiv \bar{P}(z, t), \quad \text{say} \tag{2.16}$$

of these equations satisfies the conservation law

$$\int_{-\infty}^{\infty} \bar{P}\, dz = \begin{cases} 1 & (t \geqslant 0) \\ 0 & (t < 0) \end{cases} \tag{2.17}$$

Insofar as the effective use of computer resources is concerned, the one-dimensional Taylor Aris macroscale equation (2.11) for computing $\bar{P}(z, t)$ – albeit valid only for the long times t indicated in (2.10) – is obviously far superior to the *ab initio* scheme embodied in the numerical solution of the three-dimensional microscale convective-diffusive equation (2.11) [leading to $\bar{P}(z, t)$ via (2.9)]. Moreover, the existence, functional dependence upon microscale parameters in Fig. 2, and physical interpretation of the macrotransport coefficients $\bar{U}^*$ and $\bar{D}^*$ as representing the mean axial solute velocity and dispersivity about the mean, obviously furnish useful physical insights into the global aspects of the transport process. Comparable insight would clearly be absent from the purely numerical "first principles" solution of the microscale equation (2.11) leading to $\bar{P}$ for some specific initial position (r', ϕ', z').

2.3. Taylor–Aris Paradigm

The (generalized) Taylor–Aris paradigm[30] ultimately resulting in the expressions (2.12) and (2.13) for the macrotransport coefficients $\bar{U}^*$ and $\bar{D}^*$ derives from asymptotically equating [for long times (2.10), and for each integer value $m = 0, 1, 2, \ldots$] the axial moments (2.8) of the microfield $P(r, \phi, z, t)$ with the comparable axial moments,

$$\bar{M}_m \overset{\text{def}}{=} \pi r_o^2 \int_{\infty}^{\infty} (z - z')^m\, \bar{P}\, dz \tag{2.18}$$

of the macrofield $\bar{P}(z, t)$. More explicitly, the theory involves asymptotically matching $\bar{M}_m(t)$ with $M_m(t)$ insofar as dominant-order algebraic terms in t are concerned. Such dominant asymptotic matching is possible independently of the initial cross-sectional position (r', ϕ') (and z') at which the tracer solute molecule is introduced. [The physical basis for this independence is explained in the paragraph following Eq. (2.21).]

2.4. Lagrangian Interpretation of $\bar{U}^*$ and $\bar{D}^*$

The convective-dispersion equation (2.11) asymptotically satisfied by the probability density (2.9) constitutes a *Eulerian* form of the macrotransport equation governing axial transport of the solute molecule. In what follows we consider an alternative *Lagrangian* interpretation of this equation, or, more precisely, of the phenomenological coefficients $\bar{U}^*$ and $\bar{D}^*$ appearing therein. Toward this end, consider the first axial moment M_1 of P, namely

$$\overline{z - z'} \stackrel{\text{def}}{=} \int_{z'} \int_0^{2\pi} \int_0^{r_0} (z - z')\, Pr\, dr\, d\phi\, dz \tag{2.19}$$

as well as the second (central) axial moment, $M_2 - M_1 M_1$, of P, namely

$$\overline{(z - \bar{z})^2} \stackrel{\text{def}}{=} \int_{z'} \int_0^{2\pi} \int_0^{r_0} (z - \bar{z})^2\, Pr\, dr\, d\phi\, dz \tag{2.20}$$

2.4.1. Mean Solute Velocity $\bar{U}^*$. Physically, (2.19) represents the mean axial displacement (at time t) of the solute molecule from the original axial position z' at which it was originally introduced into the system. For sufficiently long times satisfying the inequality (2.10) it can be shown[5,31] that the right-hand side of (2.19) grows linearly with time; explicitly,

$$\overline{z - z'} \simeq \bar{U}^* t \tag{2.21}$$

where $\bar{U}^*$ is a constant, independent of t [as well as of the solute's initial position (r', ϕ', z')]. The quantity $\bar{U}^*$ appearing in this asymptotic displacement formula may be interpreted as the mean axial velocity of the tracer, in the Lagrangian sense described in the following paragraph.

Due to its (lateral) Brownian motion the solute tracer molecule is able to cross the streamlines of the Poiseuille flow, moving stochastically from one to the other, as in Fig. 3. Instantaneously, while situated at the radial position r, the tracer is conveyed axially with the same local Poiseuille velocity $v(r)$ as the carrier fluid (the solvent). For times obeying the dimen-

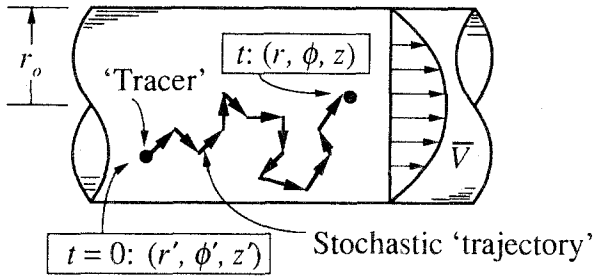

Fig. 3. Stochastic "trajectory" of a Brownian tracer or "molecule" initially introduced at time $t = 0$ into the system at the point (r', ϕ', z') and currently present at time t at the point (r, ϕ, z).

sionless inequality (2.10) the solute molecule will have sampled many times (by lateral diffusion) all transverse positions r (and ϕ) in the tube cross section, and hence have sampled each of the prevailing axial velocities $v(r)$ a statistically significant number of times. As a result, the tracer will, on average, move axially with a mean velocity $\bar{U}^*$ which is independent of the initial cross-sectional position r' (and ϕ') at which it was originally introduced. The solute velocity $\bar{U}^*$ is obviously stochastically formed from all of the instantaneous velocities $v(r)$ sampled by the tracer during its random-walk cross-sectional sojourns as it is simultaneously being carried downstream by the Poiseuille flow of the solvent. Thus (see Fig. 4), the solute molecule will, on average, traverse the axial distance $L \equiv z - z'$ in time t [from a point (r', ϕ') on the inlet plane z' to a point (r, ϕ) on the exit plane $z = z' + L$]. In a Lagrangian sense,[31] namely, involving tracking

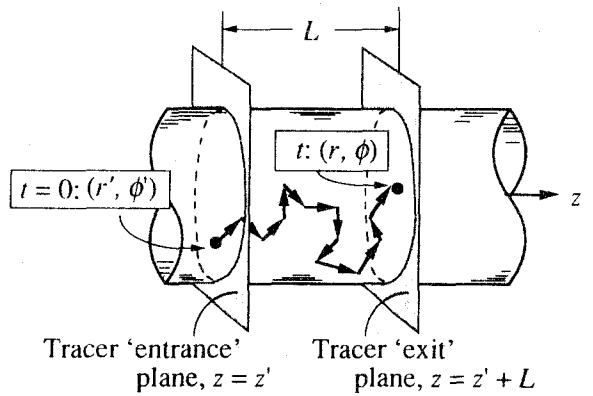

Fig. 4. Downstream stochastic motion of a Brownian tracer "molecule." The latter enters the system at the "entrance" plane $z = z'$ at time $t = 0$ and leaves the system across the "exit" plane $z = z' + L$ at time t.

the particle position in time, the mean axial velocity $\bar{U}^*$ of the solute is thus given by the relation $\bar{U}^* = L/t$.

Taylor's first relation, Eq. (2.12), namely $\bar{U}^* = \bar{V}$, corresponds to equality of the mean solute and solvent velocities down the tube. This seemingly obvious fact should, however, be regarded as nontrivial, as the velocity $\bar{U}^*$ refers to the mean solute velocity in a Lagrangian sense, namely following the tracer's motion in time, whereas the mean fluid velocity $\bar{V}$ refers to the *Eulerian* (i.e., areal) mean solvent velocity (2.2) at a fixed tube cross section, $z = \text{const}$. In order to understand Taylor's velocity equality it is thus necessary to also think kinematically of the mean stochastic *Lagrangian* motion of a *solvent* molecule in time as it moves axially, radially, and azimuthally through the tube. The essence of (2.12) is then that, on average, a (point-size) solute molecule behaves identically to a solvent molecule in a kinematical sense—at least in the present problem, where no biasing forces exist insofar as cross-sectional positions (r, ϕ) of the solute molecule are concerned; that is, in the long run [where the temporal inequality (2.10) obtains] all transverse positions in the tube cross section are equally likely for the solute molecule. By allowing sufficient time for these transverse positions to be sampled, the solute molecule will "forget" the initial cross-sectional position (r', ϕ') at which it was introduced into the tube.

We have emphasized the equality $\bar{U}^* = \bar{V}$ of solute and solvent mean velocities because such equality is not generally to be expected. Indeed, it will be seen later that differences generally exist between these two velocities whenever biases exist in the lateral positions (r, ϕ) accessible to a solute molecule. Such mean velocity disparities ultimately provide a basis for the chromatographic separation of solutes arising from differences in their cross-sectional biases.

2.4.2. Dispersivity $\bar{D}^*$. For times t satisfying the inequality (2.10), namely $t \gg r_o^2/D$, it can be shown[5,31] that the second central axial moment (2.20) grows linearly with time; explicitly,

$$\overline{(z - \bar{z})^2} \simeq 2\bar{D}^* t \tag{2.22}$$

where $\bar{D}^*$ is a constant, independent of t (as well as of r', ϕ', and z'), given explicitly by Taylor's second relation, Eq. (2.13). Analogous to Einstein's celebrated Brownian motion relation, namely $\overline{(\Delta z)^2} = 2Dt$ for the mean-square unidirectional displacement of a solute molecule diffusing (with molecular diffusivity D) through the *quiescent* solvent, Eq. (2.22) gives the dispersion about the mean solute position $\bar{z}$ $(\equiv z' + \bar{U}^* t)$ at time t in the *flowing* solvent. However, in contrast with Einstein's mean-square displacement relation, which is exact for all times t, Eq. (2.22) is only

asymptotically valid after the solute molecule has had an opportunity to sample (many times) all of the Poiseuille velocities $v(r)$ in the tube cross section.

The Einstein-like *Lagrangian* interpretation (2.22) of the dispersivity $\bar{D}^*$ contrasts with the classical *Eulerian* Fick's-law total axial flux interpretation of $\bar{D}^*$ implicit in the macroscale conservation law (2.11). Refering to Fig. 3, this dispersion arises from the fact that due to the stochastic nature of the molecular Brownian motion, not all solute molecules originally introduced at the inlet plane z' will cross the distant exit plane z ($\equiv z' + L$) at the same time [even if they are introduced simultaneously at the same cross-sectional location (r', ϕ')]. Rather, there will exist a distribution of arrival times at the exit plane about the mean time $t = L/\bar{U}^*$. In particular, the leading term of (2.13) represents the contribution to this dispersion resulting from the solute's *axial* molecular diffusion, whereas the second (generally more dominant) term arises from the solute's *transverse* molecular diffusion. The latter contribution is highly nonlinear, resulting from microscale interaction between lateral Brownian motion and axial convection. Taylor[1,2] himself explains why this contribution to the dispersion is greater the smaller is the (transverse) molecular diffusivity.

2.5. Generalized Taylor Dispersion Theory. Macrotransport Processes

The same single-particle Lagrangian approach embodied in the archetypal tube-flow problem can be applied to large classes of microscale convective-diffusive-reactive transport phenomena governed by linear constitutive equations and boundary conditions, leading to generalized Taylor dispersion theory.[5,6] More recently, this subject has been termed *macrotransport processes.*[32] A representative sampling of illustrative problems is addressed in subsequent sections. For simplicity of presentation these have all been selected as constituting simple variants of the original Taylor–Aris problem.

3. FINITE-SIZE SPHERE. HYDRODYNAMIC CHROMATOGRAPHY

The preceding Taylor–Aris tube-flow analysis has been extended[25,27] from an effectively point-size solute molecule to a finite-size colloidal Brownian sphere (radius a). Hydrodynamic and steric wall effects resulting from the nonzero value of the parameter $\lambda = a/r_o$ represent the unique features of this problem, leading ultimately to a "steric exclusion" chromato-

graphic scheme pioneered by Small[33] for separating colloidal spherical particles of different sizes via Poiseuille flow in capillary tubes.

Imagine that the Brownian sphere undergoing transport is composed of a transparent material possessing the same refractive index as the solvent in which it is suspended, thereby rendering the sphere invisible to an observer. Suppose now that a point-size black dot is placed at the center of the sphere, so that this point constitutes the only object within the solvent visible to the observer. The stochastic trajectory of this body-fixed point (termed the particle "locator point") will then represent the entire sphere's motion through the solvent. Being a point, to which classical continuum-mechanical principles can be applied, one may now calculate the conditional probability density $P(r, \phi, z, t \mid r', \phi', z')$ that the sphere center is situated at the point (r, ϕ, z) at time t, given that it was initially situated at the position (r', ϕ', z') at time $t = 0$.

The microscale conservation equation governing transport of the finite-size sphere (center) through the circular cylinder differs in the values of its phenomenological functions from the comparable point-size convective-diffusion equation (2.4) owing to the existence of wall effects arising from the nonzero value of λ. In particular, (2.4) is here replaced by

$$\frac{\partial P}{\partial t} + U(r)\frac{\partial P}{\partial z} = \nabla \cdot [\mathbf{D}(r)\,\nabla P] \tag{3.1}$$

where $U(r)$ is the axial velocity with which a neutrally-buoyant force- and couple-free sphere of radius a (whose center is situated at r) would move when suspended in the (undisturbed) Poiseuille flow (2.1) of the mean solvent velocity $\bar{V}$. Due to wall effects, the translational molecular diffusivity $\mathbf{D}(r)$ of the sphere is no longer a position-independent scalar as in (2.4), but is now rather a second-rank tensor whose value depends upon the radial position r of the sphere center within the tube.

Assuming the pertinent phenomenological functions to be known, Eq. (3.1) may, in principle, be solved subject to the respective initial- and boundary-value conditions (2.5) and (2.7), and with (2.6) here replaced by the no-flux condition

$$\partial P/\partial r = 0 \qquad \text{at} \quad r = r_o - a \tag{3.2}$$

The latter reflects the fact that owing to the sphere's finite radius a, the sphere center is sterically excluded from the annular domain

$$r_0 - a < r < r_o \tag{3.3}$$

adjacent to the wall, and is hence only able to sample those points lying within the circular cylindrical domain

$$0 \leqslant r < r_o - a \tag{3.4}$$

of radius $r_o - a$.

Using available wall-effect data for the phenomenological functions $U(r)$ and $\mathbf{D}(r)$ required in (3.1), the generalized Taylor dispersion theory paradigm eventually yields[25] for the mean solute velocity[4] $\bar{U}^*$

$$\frac{\bar{U}^*}{\bar{V}} = 1 + 2\lambda - 4.9\lambda^2 + O(\lambda^3) \qquad (\lambda \ll 1) \tag{3.5}$$

This expression is valid only for the case

$$\lambda \lesssim 0.20 \quad \text{(approx.)} \tag{3.6}$$

owing to the current unavailability of the phenomenological functions required in (3.1) for larger values of λ. Equation (3.5) is plotted in Fig. 5.

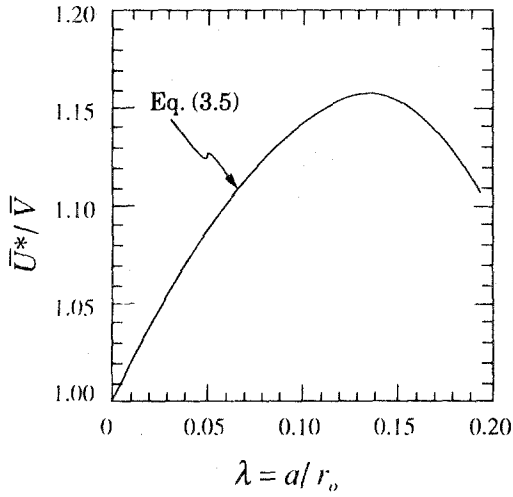

Fig. 5. Mean axial velocity $\bar{U}^*$ of a neutrally buoyant Brownian sphere of radius a transported by a Poiseuille flow (mean velocity $\bar{V}$) through a circular capillary tube of radius r_o.

[4] While $\bar{U}^*$ represents the mean velocity of the *center* of the finite (and rotating) sphere, it also represents the mean velocity of the sphere itself since, for long times, *all* points lying within the sphere interior will, on average (owing to the inequality $L \gg a$), have traveled the same axial distance L down the tube (cf. Fig. 4).

Similar calculations performed for the dispersivity may be expressed in the form

$$\bar{D}^* = \bar{D}^M + \bar{D}^C \tag{3.7}$$

where the "hindered" diffusivity $\bar{D}^M$ (cf. Fig. 6) of the Brownian sphere through the *quiescent* solvent is[25]

$$\frac{\bar{D}^M}{D_\infty} \simeq \frac{1-(9/8)\lambda \ln(\lambda^{-1}) - 1.539\lambda + O(\lambda^2)}{(1-\lambda)^2} \qquad (\lambda \ll 1) \tag{3.8a}$$

valid for the values of λ indicated in (3.6), whereas[27]

$$\frac{\bar{D}^M}{D_\infty} \simeq 0.984\varepsilon^{5/2} + O(\varepsilon^3) \qquad (1-\lambda \ll 0) \tag{3.8b}$$

for the large, closely-fitting, sphere case, with

$$\varepsilon = \frac{r_o - a}{a} \equiv \frac{1}{\lambda} - 1 \ll 0 \tag{3.9}$$

a small, dimensionless, gap-width parameter. Here, D_∞ is the diffusivity of the Brownian sphere in the *unbounded* solvent, given typically by the Stokes–Einstein equation $D_\infty = kT/6\pi\mu_o a$, with kT the Boltzmann factor

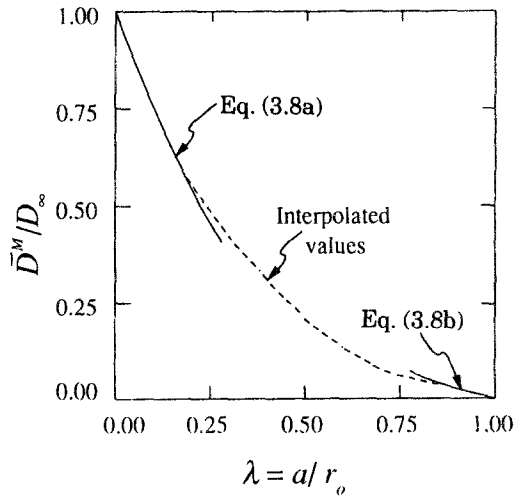

Fig. 6. Hindered mean axial molecular diffusivity $\bar{D}^M$ of a Brownian sphere of radius a through a quiescent viscous solvent confined within a circular capillary tube of radius r_o.

and μ_o the solvent viscosity. The Taylor or "convective" contribution $\bar{D}^C$ is[25]

$$\bar{D}^C = \frac{r_o^2 \bar{V}^2}{48 D_\infty} \left[\frac{1 - 3.862\lambda + 14.40\lambda^2 + O(\lambda^3)}{(1-\lambda)^2} \right] \qquad (\lambda \ll 1) \qquad (3.10)$$

Several important features appear in Eq. (3.5) for the mean velocity of the sphere, the most interesting of which is that (since $\bar{U}^* > \bar{V}$) the sphere moves faster on average than does the solvent in which it is suspended. This conclusion stems from the fact that because of the condition of impenetrability of the tube wall, the sphere center is unable to sample those points lying within the annular region (3.3) adjacent to the tube wall, where the slower-moving Poiseuille flow streamlines obtain [cf. Eq. (2.1)]. Thus, in contrast with the solvent molecules, which sample *all* cross-sectional points equally, the solute molecule does not "waste its time" in these slow-moving streamlines; that is, the sphere (center) samples only the faster-moving streamlines, away from the wall. It is for this reason that a spherical solute molecule comparable in radius to that of the capillary tube moves faster on average than do the (point-size) solvent molecules composing the fluid continuum. [Though this steric exclusion effect is offset to some extent by the retarding hydrodynamic effect of the tube wall upon the finite-size sphere, the "cutoff" of the slower-moving Poiseuille flow streamlines in the annular region (3.3) constitutes the dominant effect upon $\bar{U}^*$. Indeed, the steric factor of $+2\lambda$ in Eq. (3.5) arises from this cutoff,[5] whereas the $-4.9\lambda^2$ hydrodynamically-induced term arises from the retarding effect of the wall. And, as the latter is of higher order in λ than the former, it is of less importance in the $\lambda \ll 1$ limit.]

Equation (3.5) and Fig. 5 show that, all other things (namely r_o and $\bar{V}$) being equal, the larger the sphere radius a, the faster the sphere moves (at least for $\lambda \lesssim 0.15$). The simple reason for this is the larger is a, the greater is the number of slower-moving streamlines within the annular region (3.3) rendered inaccessible to the sphere center. This phenomenon provides a basis for the chromatographic separation of a (dilute) mixture of Brownian spheres of different radii a_i, since these will travel, on average, at different axial speeds $\bar{U}_i^*$ $(i = 1, 2, \ldots)$. This phenomenon was termed "*hydrodynamic chromatography*" by Small,[33] who first experimentally demonstrated its existence.

[5] That is, using (2.1),

$$\frac{1}{\pi r_o^2} \int_0^{2\pi} \int_0^{r_o - a} v(r) r \, dr \, d\phi = (1 + 2\lambda) \bar{V}$$

That no weighting factor appears in the integrand of the latter stems from the fact that, due to the transverse Brownian motion of the sphere, the sphere center samples all points equally in the circular domain (3.4).

Figure 7 schematically depicts the hydrodynamic chromatographic separation of an initially uniform mixture composed of two different sphere sizes (respectively characterized by the radii $a_2 > a_1$), on the assumption that the mixture is so dilute that no hydrodynamic or other interaction occurs among the solute spheres comprising the mixture. The peaks, corresponding to maxima in the two solute concentrations, move at respective velocities $\bar{U}_2^* > \bar{U}_1^* > \bar{V}$. The effect of the dispersion about these peaks, quantified by the respective dispersivities $\bar{D}_2^*$ and $\bar{D}_1^*$, is to decrease the *sharpness* of the separation between the two species.

Knowledge of the functional dependences of $\bar{U}_i^*$ and $\bar{D}_i^*$ $(i = 1, 2, \ldots)$ upon the fundamental parameters of the system (namely, r_o, $\bar{V}$, a_i, D_i) for each of the solute species i being separated permits a complete engineering design of the chromatographic separation system. In practice, of course, one often uses (monodisperse) packed beds rather than simple capillary tubes to effect this separation. One must then resort to additional geometrical modeling, involving—in the simplest case—use of an "effective radius" r_o for the characteristic size of the packed-bed interstitial pore space; more realistic geometrical models of packed beds—typically spatially-periodic models[12,34]—have also been the subject of generalized Taylor dispersion theory analyses.

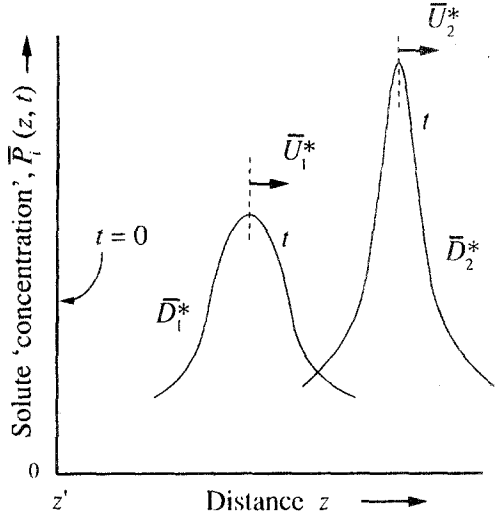

Fig. 7. Chromatographic separation (in a circular capillary tube) of an initially uniform mixture introduced into the flowing fluid at the plane $z = z'$ at time $t = 0$. At time t the two species, which respectively move at the different mean axial velocities $\bar{U}_1^*$ and $\bar{U}_2^*$, have separated into two diffuse "bands." The diffuseness embodied in these bands, which limits the sharpness of the separation, arises from the respective dispersivities $\bar{D}_1^*$ and $\bar{D}_2^*$ of the two species.

4. SOLUTE ADSORPTION ON THE WALLS. AFFINITY CHROMATOGRAPHY

Returning to the original Taylor–Aris-type analysis of Section 2, involving a *point-size* Brownian solute molecule suspended in a Poiseuille flow within a circular capillary tube, consider the case where the solute molecule experiences absorption forces tending to deposit it on the tube walls.[11,35] In the simplest possible case the previous Taylor–Aris microscale no-flux boundary condition (2.6) is here replaced by the linear Henry's law adsorption isotherm

$$p = kP\,|_{r=r_o} \tag{4.1}$$

with k the Henry's law constant and p the surface-excess solute "concentration" (probability density) on the wall, measured in amount of solute per unit area. In its adsorbed state the solute may diffuse along the wall with a surface diffusivity D^s in addition to undergoing both diffusion in the bulk fluid (with molecular diffusivity D) and Poiseuille flow convection (with mean velocity $\bar{V}$).

With[6]

$$K = 2k/r_o \tag{4.2}$$

a dimensionless Henry's law constant, application of the generalized Taylor dispersion theory paradigm derived from the Lagrangian equations (2.21) and (2.22) eventually yields

$$\frac{\bar{U}^*}{\bar{V}} = \frac{1}{1+K} \tag{4.3}$$

for the mean axial solute velocity $\bar{U}^*$, and Eq. (3.7) for the total axial solute dispersivity required in (2.11). Here,

$$\bar{D}^M = \frac{D + KD^s}{1+K} \tag{4.4}$$

[6] The inverse length factor $2/r_o$ appearing in (4.2) represents the so-called specific surface of the capillary tube; that is, for an arbitrary axial length l of capillary, it represents the ratio

$$\frac{2\pi r_o l}{\pi r_o^2 l} = \frac{2}{r_o}$$

corresponding to the wetted surface area per unit volume. This factor arises naturally in adsorption problems when the areal results are expressed on a volumetric macroscale basis, as in Eq. (2.11).

is the purely molecular contribution (corresponding to the quiescent fluid case), and

$$\bar{D}^c = \frac{r_o^2 \bar{V}^2}{48D} \frac{1 + 6K + 11K^2}{(1+K)^3} \tag{4.5}$$

is the Taylor or convective contribution.

Since $K > 0$, Eq. (4.3) reveals that, on average, the solute molecule moves through the tube more slowly than does a comparable solvent molecule, i.e., $\bar{U}^* < \bar{V}$. This phenomenon arises here because the (short-range) adsorptive forces acting upon the solute molecule when in proximity to the tube wall cause it to spend a disproportionately large fraction of its time in that neighborhood, where the slower-moving Poiseuille flow streamlines prevail. In other words, whereas a solvent molecule is free to sample, without bias, all points in the tube cross section, the solute molecule is biased in favor of the slower-moving streamlines proximate to the wall. By favoring these streamlines, a solute molecule thus moves, on average, more slowly in the axial direction than does a solvent molecule.

Equation (4.3) points up the possibility of chromatographically separating two (or more) solute species possessing different adsorptivities k_i ($i = 1, 2, \ldots$). Thus, if K_1 and K_2 are the dimensionless adsorptivities (4.2) of solutes 1 and 2, their respective mean velocities down the tube will be in the ratio

$$\frac{\bar{U}_1^*}{\bar{U}_2^*} = \frac{1 + K_2}{1 + K_1} \equiv \frac{r_o + 2k_2}{r_o + 2k_1} \tag{4.6}$$

This yields the inequality $\bar{U}_1^* > \bar{U}_2^*$ whenever $k_1 < k_2$, so that the least strongly-bound species (i.e., species "1") is the faster moving of the two. Equation (4.6) provides the basis for understanding *affinity chromatography*, whereby the separation of solutes possessing different affinities k is accomplished by virtue of their different mean velocities. The ensuing chromatographic separation of the two species is similar to that depicted schematically in Fig. 7.

Equation (4.4) for the macroscale or effective molecular diffusivity $\bar{D}^M$ embodies respective contributions from both the volumetric (D) and surface (D^s) molecular diffusion processes. This corresponds physically to these processes operating in *parallel*. Whenever $D^s > D$, the overall molecular diffusion process through the quiescent solvent occurs more rapidly than would otherwise occur for pure bulk transport, and conversely.

5. CHEMICALLY REACTIVE SOLUTE

Consider the case where the (point-size) formerly passive solute of Section 2 now undergoes a first-order irreversible chemical reaction at the tube wall (e.g., a catalyst is present there). In this situation the Taylor–Aris microscale no-flux condition (2.6) at the tube wall is here replaced by the (linear) boundary condition

$$-D\frac{\partial P}{\partial r}=kP \qquad \text{at} \quad r=r_o \tag{5.1}$$

with k the reaction-velocity constant. In such circumstances solute is no longer conserved (as a chemical species). Rather, upon reaching the wall (via Brownian motion) a solute molecule may be permanently removed from the bulk fluid as a result of undergoing chemical reaction.

The previous Eulerian macrotransport equation (2.11) governing the long-time transport of the macroscale solute density $\bar{P}$ of (2.9) is replaced in the present circumstances by the expression[21,22,36]

$$\frac{\partial \bar{P}}{\partial t}+\bar{U}^*\frac{\partial \bar{P}}{\partial z}\simeq \bar{D}^*\frac{\partial^2 \bar{P}}{\partial z^2}-\bar{K}^*\bar{P} \tag{5.2}$$

The microscale first-order irreversible *surface* chemical reaction (5.1) occurring at the wall thus manifests itself at the macroscale as a first-order irreversible *volumetric* chemical reaction (characterized by the bulk reaction-velocity constant $\bar{K}^*$).

Surprisingly, the mean velocity $\bar{U}^*$ with which the reactive solute moves axially is not the same as the mean solvent velocity $\bar{V}$. As such, the solute is not simply convected on average with the inert carrier; rather, the solute moves *faster* than does the fluid; explicitly, $\bar{U}^*>\bar{V}$. This phenomenon stems from the fact that only those solute molecules "smart enough" to stay away from the wall region survive their trip downstream, thus enabling them to accomplish the transit from tube entrance to exit; conversely, those molecules "foolish" enough to meander (by lateral Brownian motion) over to the tube wall are destroyed by the reaction. As such, those solute molecules that exit the tube (and are hence counted in the entrance/exit scheme depicted in Fig. 4) have not sampled the slower-moving streamlines of the Poiseuille flow existing near to the wall; stated alternatively, those molecules surviving the trip downstream, and hence exiting the tube, have on average sampled only the faster-moving streamlines distant from the tube wall. In contrast, the (inert) solvent molecules (*all* of which survive the trip downstream) sample all cross-sectional points and hence all streamlines in the tube equally, in effect "wasting" a portion of their time in the slowest-moving streamlines.

The exact amount by which $\bar{U}^*$ exceeds $\bar{V}$ depends upon the Damkohler number[7]

$$\mathbf{Da} = \frac{kr_o}{D} \tag{5.3}$$

In a similar vein, $\bar{D}^* = \bar{D}^M + \bar{D}^C$, where $\bar{D}^M = D$, as before; however, $\bar{D}^C$ does not possess the same classical Taylor value (2.13) for a passive solute as it does for a reactive solute; rather, the ratio $\bar{D}^C/\bar{D}_0^C$ (where the denominator $\bar{D}_0^C$ denotes the classical Taylor value, $r_o^2\bar{V}^2/48D$) will also depend upon the Damkohler number (5.3), the rather complex functional dependence being given explicitly by Shapiro and Brenner.[21]

Of course, the effective macroscale volumetric reaction velocity constant $\bar{K}^*$ (in the dimensionless form $\bar{K}^* r_o/k$) is also functionally dependent upon the Damkohler number. For small values of the latter, one finds that

$$\bar{K}^* = 2\frac{k}{r_o} \qquad (\mathbf{Da} \ll 1) \tag{5.4}$$

In this *kinetically-controlled* limit, diffusive transport to the reactive wall occurs sufficiently rapidly such that the effective reactivity is governed solely by the true chemical kinetics, as quantified by the microscale reaction-velocity constant k. [In this context note that the factor of

[7] The exact relation is[21]

$$\frac{\bar{U}^*}{\bar{V}} = 1 + \frac{1 + (\beta_0 \mathbf{Da}^{-1} - 2\beta_0^{-1})^2}{3[(\beta_0 \mathbf{Da}^{-1})^2 + 1]}$$

where $\beta_0 \equiv \beta_0(\mathbf{Da})$ is the smallest positive root of the transcendental equation[37]

$$\beta J_1(\beta) - \mathbf{Da}\, J_0(\beta) = 0$$

with J_n the Bessel function of order n. In the limit of small and large **Da**, the respective asymptotic roots of the latter equation are, respectively,

$$\beta_0 \simeq 2\mathbf{Da} \qquad (\mathbf{Da} \ll 1)$$

and

$$\beta_0 \simeq 2.4048 \qquad (\mathbf{Da} \gg 1)$$

the 2.4048 coefficient being the smallest positive root of the equation $J_0(\beta) = 0$.

For later reference we also note that, in general,

$$\bar{K}^* = \beta_0^2 D/r_o^2$$

for arbitrary **Da**.

$2/r_o$ appearing in (5.4) corresponds to the so-called specific surface of the circular cylindrical tube, as previously observed in connection with Eq. (4.2).] In the opposite, *diffusion-controlled*, limit one obtains

$$\bar{K}^* = 5.783 \frac{D}{r_o^2} \qquad (\mathbf{Da} \gg 1) \tag{5.5}$$

(See the preceding footnote for the source of the 5.783... coefficient.) Here, the effective reaction rate is limited by the ability of the solute to diffuse to the wall.

Finally, we observe that despite the fact that the phenomenological coefficients $\bar{U}^*$, $\bar{D}^*$, and $\bar{K}^*$ appearing in the reactive macrotransport equation (5.2) are independent of the initial microscale data [i.e., of the initial cross-sectional position (r', ϕ') at which the solute molecule is introduced into the system at time $t=0$], the macroscale conditional probability density $\bar{P}$, defined by (2.9), will nevertheless depend upon this initial condition—explicitly upon r'. The reason for this derives from the fact that the macrotransport equation (5.2) governing $\bar{P}$, rather than being *exactly* true for all times t, is only valid asymptotically for times t satisfying the transverse sampling-time criterion (2.10). And, for earlier times, namely $t \leqslant O(r_o^2/D)$, *preceding that for which the macroscale description (5.2) becomes valid*, a solute molecule initially introduced too near the reactive wall will have a higher probability of being destroyed by chemical reaction than one introduced further from the wall. Thus, not all solute molecules initially introduced into the system survive long enough for the macrotransport equation (5.2) to henceforth become a valid descriptor of their fate.

As a result of these facts, in order that the value (2.9) of $\bar{P}$ [derived by "first-principles" quadrature from the microscale solution P of Eqs. (2.4), (2.5), (2.7), and (5.1)] asymptotically match the comparable solution $\bar{P}$ of the macroscale equation (5.2) [subject to the far-field boundary condition (2.14)], one must subject the solution of the latter to a *fictitious* initial condition, say $\bar{P}(z, 0)$, at $t=0$ in place of the true initial condition (2.15). The scheme for deriving this fictitious initial condition from the given microscale phenomenological data, namely $v(r)$, $\bar{V}$, r_o, D, and k (as well as r'), is discussed by Shapiro and Brenner.[21 23]

Practical packed-bed reactor design principles may need to be reexamined in view of the significant differences observed here between macroscale descriptions of passive vs. reactive solute transport processes. In particular, residence-time distribution-type analyses (especially of first-order irreversible chemical reactions) appear to be conceptually inappropriate in situations for which the reaction-velocity constant is nonuniform

across the tube cross section,[22] such as is the case here when it is nonzero only at the tube wall, $r = r_o$.

6. AEROSOL DEPOSITION

As a final example, we consider the case of a Brownian aerosol or hydrosol solute particle being deposited (from a dilute suspension of noninteracting particles) upon the walls of the capillary tube within which a Poiseuille flow occurs at mean velocity $\bar{V}$.[24] Assuming that such a submicron particle, upon reaching the wall, is held there permanently by (short-range) attractive forces, the Taylor–Aris microscale no-flux condition (2.6) at the tube wall is here replaced by the boundary condition[38]

$$P = 0 \qquad \text{at} \quad r = r_o \tag{6.1}$$

The wall thus functions as a sink for any solute particle reaching it (by lateral Brownian motion). As a result of its removal from the bulk fluid, solute is not conserved (as a chemical species) at the macroscale.

The situation here is entirely analogous to the microscale first-order irreversible surface chemical reaction case of Section 5 in the limiting situation where the reaction-velocity constant $k \to \infty$. As a result of this analogy, the basic aerosol macrotransport equation is given by (5.2), in which the effective volumetric reactivity coefficient is [cf. Eq. (5.5)]

$$\bar{K}^* = 5.783 \frac{D}{r_o^2} \tag{6.2}$$

This macroscale phenomenological coefficient quantifies the rate of solute disappearance from the bulk fluid, and hence quantifies the corresponding rate of solute deposition upon the tube wall. Thus, whereas no real chemical reaction occurs at the microscale it nevertheless appears at the macroscale, as if a first-order irreversible bulk-phase reaction is, in fact, occurring.

Based upon the microscale surface chemical reaction analogy with the results of Section 5, it follows that, on average, an aerosol particle will move axially through the tube at a mean velocity $\bar{U}^*$ exceeding the mean velocity $\bar{V}$ of the carrier fluid. Explicitly, we find that[8]

$$\bar{U}^*/\bar{V} = 1.564 \tag{6.3}$$

[8] This derives from the $\bar{U}^*/\bar{V}$ formula cited in footnote 7, upon there setting $\beta_0 = 2.4048$ and letting $\mathbf{Da} \to \infty$.

The dispersivity $\bar{D}^*$ can analogously be obtained as a limiting case of the results of Section 5 as $\mathbf{Da} \to \infty$.

Of course, to obtain the correct solution $\bar{P}$ of the aerosol macrotransport equation (5.2) one must again introduce the idea of a *fictitious* initial condition, as discussed in the preceding section.

7. CLOSURE

Given the implicit restrictions imposed by the nature of this review, we have only barely touched upon the power of macrotransport analyses in the macroscale modeling and physical interpretation of large classes of microscale convective-diffusive-reactive transport processes. Some of these processes are cited in the Introduction. Contained therein will be found references to the works of other researchers who have contributed to the development of the subject, and whose absence from our list of literature citations is regrettable.

ACKNOWLEDGMENTS

Many of our research activities pertaining to *macrotransport processes* were supported by the National Science Foundation, the Office of Basic Energy Sciences of the Department of Energy, the U.S. Army Research Office, and the Microgravity Science and Applications Division of the National Aeronautics and Space Administration, to all of whom the author is grateful for their support and encouragement.

A portion of this manuscript was written while on sabbatical leave as Chevron Visiting Professor of Chemical Engineering at the California Institute of Technology. Their support and hospitality were much appreciated. During this period I was also the recipient of a Guggenheim Memorial Foundation Fellowship.

REFERENCES

1. G. I. Taylor, Dispersion of soluble matter in solvent flowing slowly through a tube, *Proc. R. Soc. Lond. A* **219**:186–203 (1953).
2. G. I. Taylor, Conditions under which dispersion of a solute in a stream of solvent can be used to measure molecular diffusion, *Proc. R. Soc. Lond. A* **225**:473–477 (1954).
3. R. Aris, On the dispersion of a solute in a fluid flowing through a tube, *Proc. R. Soc. Lond. A* **235**:67–77 (1956).
4. R. B. Bird, W. E. Stewart, and E. N. Lightfoot, *Transport Phenomena* (Wiley, New York, 1960).
5. H. Brenner, A general theory of Taylor dispersion phenomena, *PhysicoChem. Hydrodynam.* **1**:91–123 (1980).

6. H. Brenner, A general theory of Taylor dispersion phenomena II. An extension, *Physico-Chem. Hydrodynam.* **3**:139–157 (1982).
7. H. Brenner, Taylor dispersion in systems of sedimenting nonspherical Brownian particles: I. Homogeneous, centrosymmetric, axisymmetric particles, *J. Colloid Interface Sci.* **71**:189–208 (1979).
8. H. Brenner, Taylor dispersion in systems of sedimenting nonspherical Brownian particles: II. Homogeneous ellipsoidal particles, *J. Colloid Interface Sci.* **80**:548–588 (1981).
9. H. Brenner, Dispersion resulting from flow through spatially periodic porous media, *Phil. Trans. R. Soc. Lond. A* **297**:81–133 (1980).
10. P. M. Adler and H. Brenner, Transport processes in spatially periodic capillary networks II. Taylor dispersion with mixing vertices. *PhysicoChem. Hydrodynam.* **5**:269–285 (1984).
11. L. H. Dill and H. Brenner, A general theory of Taylor dispersion phenomena III. Surface transport, *J. Colloid Interface Sci.* **85**:101–117 (1982).
12. H. Brenner and P. M. Adler, Dispersion resulting from flow through spatially periodic porous media II. Surface and intraparticle transport, *Phil. Trans. R. Soc. Lond. A* **307**:149–200 (1982).
13. H. Brenner, A general theory of Taylor dispersion phenomena IV. Direct coupling effects, *Chem. Eng. Commun.* **18**:355–379 (1982).
14. H. Brenner, A. Nadim, and S. Haber, Long-time molecular diffusion, sedimentation and Taylor dispersion of a fluctuating cluster of interacting Brownian particles, *J. Fluid Mech.* **183**:511–542 (1987).
15. H. Nadim and H. Brenner, Longtime nonpreaveraged diffusion and sedimentation properties of flexible Brownian dumbells, *PhysicoChem. Hydrodynam.* **11**:315–339 (1989).
16. L. H. Dill and H. Brenner, A general theory of Taylor dispersion phenomena V. Time-periodic convection, *PhysicoChem. Hydrodynam.* **3**:267–292 (1982).
17. L. H. Dill and H. Brenner, Dispersion resulting from flow through spatially periodic porous media III. Time-periodic processes, *PhysicoChem. Hydrodynam.* **4**:279–302 (1983).
18. M. Shapiro and H. Brenner, Taylor dispersion in the presence of time-periodic convection phenomena. Part I. Local-space periodicity; Part II. Transport of transversely oscillating Brownian particles in a plane Poiseuille flow, *Phys. Fluids A* **2**:1731–1753 (1990).
19. A. Nadim, R. G. Cox, and H. Brenner, Taylor dispersion in concentrated suspensions of rotating cylinders, *J. Fluid Mech.* **164**:185–215 (1986).
20. S. R. Dungan and H. Brenner, Sedimentation and dispersion of nonneutrally buoyant Brownian particles in cellular circulatory flows simulating local fluid agitation, *Phys. Rev. A* **38**:3601–3608 (1988).
21. M. Shapiro and H. Brenner, Taylor dispersion of chemically reactive species: Irreversible first-order reactions in bulk and on boundaries, *Chem. Eng. Sci.* **41**:1417–1433 (1986).
22. M. Shapiro and H. Brenner, Chemically reactive generalized Taylor dispersion theory, *AIChE J.* **33**:1155–1167 (1987).
23. M. Shapiro and H. Brenner, Dispersion of a chemically reactive solute in a spatially periodic model of a porous medium, *Chem. Eng. Sci.* **43**:551–571 (1988).
24. M. Shapiro and H. Brenner, Dispersion/reaction model of aerosol filtration by porous filters, *J. Aerosol Sci.* **21**:97–125 (1990).
25. H. Brenner and L. J. Gaydos, The constrained Brownian movement of spherical particles in cylindrical pores of comparable radius: Models of the diffusive and convective transport of solute molecules in membranes and porous media, *J. Colloid Interface Sci.* **58**:312–356 (1977).
26. L. J. Gajdos and H. Brenner, Field-flow fractionation: Extensions to non-spherical particles and wall effects, *Sep. Sci. Technol.* **13**:215–240 (1978).
27. G. M. Mavrovouniotis and H. Brenner, Hindered sedimentation, diffusion and dispersion

coefficients for Brownian spheres in cylindrical pores, *J. Colloid Interface Sci.* **124**:269–283 (1988).
28. M. Shapiro, A. Oron, and C. Gutfinger, Electrostatic precipitation of charged particles from turbulent flows, *J. Colloid Interface Sci.* **127**:401–416 (1989).
29. R. Mauri and H. Brenner, Rheological properties of suspensions determined by momentum tracer methods, to be published (1991).
30. I. Frankel and H. Brenner, On the foundations of generalized Taylor dispersion theory, *J. Fluid Mech.* **204**:97–119 (1989).
31. L. H. Dill and H. Brenner, A general theory of Taylor dispersion phenomena VI. Langevin methods, *J. Colloid Interface Sci.* **93**:343–365 (1983).
32. A. Nadim, M. Pagitsas, and H. Brenner, Higher-order moments in macrotransport processes, *J. Chem. Phys.* **85**:5238–5245 (1986).
33. H. Small, Hydrodynamic chromatography, a technique for size analysis of colloidal particles, *J. Colloid Interface Sci.* **48**:147–161 (1974).
34. L. C. Nitsche and H. Brenner, Hydrodynamics of particulate motion in sinusoidal pores via a singularity method, *AIChE J.* **36**:1403–1419 (1990).
35. M. J. E. Golay, Theory of chromatography in open and coated tubular columns with round and rectangular cross-sections, in *Gas Chromatography*, D. H. Desty, ed. (Butterworths, London, 1958), p. 36.
36. R. Sankarasubramanian and W. N. Gill, Unsteady convective diffusion with interphase mass transfer, *Proc. R. Soc. Lond. A* **333**:115–132 (1973).
37. H. S. Carslaw and J. C. Jaeger, *Conduction of Heat in Solids*, 2nd ed. (Oxford University Press, Oxford, 1959), p. 493.
38. M. Shapiro, H. Brenner, and D. C. Guell, Accumulation and transport of Brownian particles at solid surfaces: Aerosol and hydrosol deposition processes, *J. Colloid Interface Sci.* **136**:552–573 (1990).